Resonant Disk Turnstile

Robert K. Zimmerman, Jr., *Member, IEEE*

***Abstract*— In this paper, the resonant disk turnstile is introduced and analyzed. The disk turnstile differs from Dicke's full-waveguide turnstile in that four of the six ports are coaxial cable ports, yielding a much more compact turnstile, which is easier to construct. The disk turnstile operation is explained as a superposition of the disk TM_{01} mode (nonradiating) and the disk TM_{11} mode which couples directly to the circular waveguide (dominant) TE_{11} mode. A useful operating fractional bandwidth of 3% is possible as compared to a Dicke turnstile bandwidth of about 6%.**

***Index Terms*—Polarization, waveguides, waveguide transitions.**

I. Introduction

ROBERT DICKE invented the waveguide turnstile network during World War II at the Massachusetts Institute of Technology (MIT) Radiation Laboratory [1]–[3]. The device was patented [4] in 1954 as a network for exciting circularly polarized waves in a circular guide. The turnstile has seen immense use in radar systems and radio-astronomy installations worldwide.

Dicke's turnstile becomes quite large at L-band and below, which prompted the author to consider how a smaller equivalent network might be realized. This resulted in the resonant disk turnstile described in this paper.

Since many readers may be unfamiliar with the waveguide turnstile, Section II serves as a brief review of the device and its scattering parameter formalism. Turnstile symmetry is discussed, which allows the device to be considered as a *pseudo two-port*. Section III introduces the modal theory of disk resonators. Odd- and even-resonance modes are identified, which can emulate the symmetry properties of Dicke's turnstile. The theory of radial waveguides is invoked to develop a simple model for the relevant modes. Section IV describes a prototype L-band turnstile and its performance agreement with the model of the previous section. Section V is a prospectus of how the disk turnstile may be used in future applications.

II. Dicke's Waveguide Turnstile

Dicke's waveguide turnstile is shown in Fig. 1. Its name comes from its clear similarity to a market turnstile. Usually the waveguide turnstile is regarded as a six-port device, with four rectangular guides, each supporting a TE_{10} mode (ports 1–4) and the round guide providing two orthogonal TE_{11} polarizations (ports 5 and 6). As quoted from [1]: "the waveguide turnstile has a fourfold symmetry axis and four symmetry planes." This is shown in Fig. 2. Due to this symmetry, Dicke has shown [1] that the scattering matrix must be of the form

$$\boldsymbol{S} = \begin{bmatrix} \alpha & \gamma & \delta & \gamma & \varepsilon & 0 \\ \gamma & \alpha & \gamma & \delta & 0 & \varepsilon \\ \delta & \gamma & \alpha & \gamma & -\varepsilon & 0 \\ \gamma & \delta & \gamma & \alpha & 0 & -\varepsilon \\ \varepsilon & 0 & -\varepsilon & 0 & \beta & 0 \\ 0 & \varepsilon & 0 & -\varepsilon & 0 & \beta \end{bmatrix}.$$

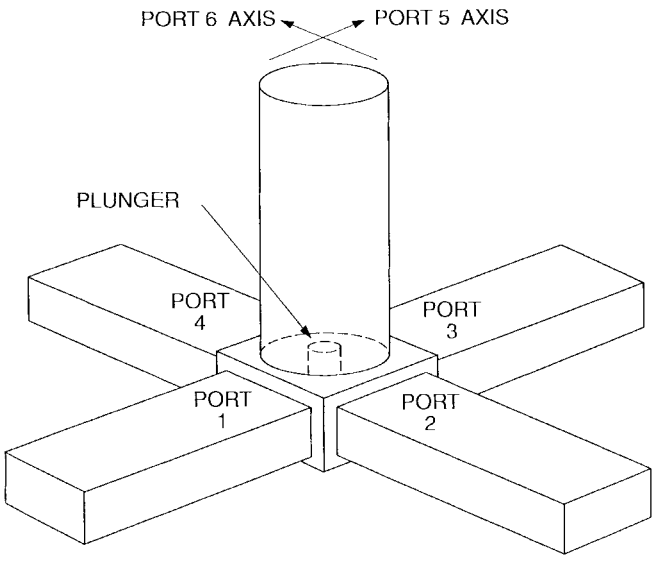

Fig. 1. Waveguide turnstile junction. Ports 1–4 are rectangular waveguides carrying the TE_{10} mode. The circular waveguide can support two orthogonal TE_{11} modes, and hence, accounts for ports 5 and 6. Port 5 couples to ports 1 and 3. Port 6 couples to ports 2 and 4.

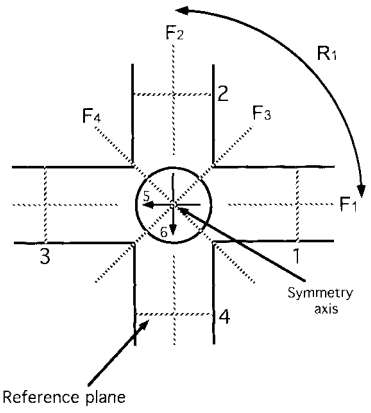

Fig. 2. Symmetry properties of the turnstile junction. The symmetry planes are F_1, F_2, F_3, andF_4. The terminal planes in the rectangular waveguide are 1, 2, 3, and 4. The terminals in the round waveguide for the two polarizations are 5 and 6. From [1].

Manuscript received February 3, 1997; revised May 19, 1997.

The author is with the Arecibo Observatory, National Astronomy & Ionosphere Center (N.A.I.C.), Cornell University, Arecibo, PR 00613 USA.

Publisher Item Identifier S 0018-9480(97)06064-X.

Note that there are only five distinct entries. For a turnstile operating at its intended center frequency (ideal operation), the entries take the values $\alpha = \beta = \delta = 0$, $\varepsilon = 1/\sqrt{2}$, $\gamma = 1/2$.

The turnstile, regarded as a six-port, has a complicated signal-flow graph which will not be presented. However, due to the symmetry of the junction, the scattering matrix takes a form which allows the network to be viewed as a two-port. For example, consider rectangular ports 1 and 3 (opposite ports). Suppose these ports are driven in-phase with each other with unit inputs. Applying the scattering matrix $\boldsymbol{S}$ yields

$$\boldsymbol{S}\begin{bmatrix}1\\0\\1\\0\\0\\0\end{bmatrix} = \begin{bmatrix}\alpha+\delta\\2\gamma\\\alpha+\delta\\2\gamma\\0\\0\end{bmatrix} = (\alpha+\delta)\begin{bmatrix}1\\0\\1\\0\\0\\0\end{bmatrix} + 2\gamma\begin{bmatrix}0\\1\\0\\1\\0\\0\end{bmatrix}.$$

For in-phase drive to ports 1 and 3, there is a reflection back to ports 1 and 3, and a forward scattered signal to ports 2 and 4. Let

$$\Gamma_{\text{even}} = \alpha + \delta$$

represent the even-drive reflection coefficient. With backward and forward scattering, this arrangement very much resembles a two-port. In fact, since ports 2 and 4 carry identical signals, these ports could be brought together in an E-plane junction so as to yield a single output port. Then the two-port picture would be complete.

In a similar manner, consider ports 1 and 3 driven out-of-phase (with respect to each other) with unit inputs. Applying the scattering matrix $\boldsymbol{S}$ yields

$$\boldsymbol{S}\begin{bmatrix}1\\0\\-1\\0\\0\\0\end{bmatrix} = \begin{bmatrix}\alpha-\delta\\0\\\delta-\alpha\\0\\2\varepsilon\\0\end{bmatrix} = (\alpha-\delta)\begin{bmatrix}1\\0\\-1\\0\\0\\0\end{bmatrix} + 2\varepsilon\begin{bmatrix}0\\0\\0\\0\\1\\0\end{bmatrix}.$$

For out-of-phase drive to ports 1 and 3, there is a reflection back to ports 1 and 3, and a forward scattered signal to port 5. Let

$$\Gamma_{\text{odd}} = \alpha - \delta$$

represent the odd-drive reflection coefficient. Here again, is the form of a two-port.

In practice, the even or odd reflection coefficient may be measured using an in-phase or out-of-phase power splitter, as shown in Fig. 3. Two-port theory may be rigorously applied to show that all five of the scattering parameter entries have simple expressions in terms of Γ_{even} and Γ_{odd}. Phase reference planes may be chosen such that the relations are as given below:

$$\begin{aligned}\alpha &= (\Gamma_{\text{even}} + \Gamma_{\text{odd}}/2\\ \beta &= \Gamma_{\text{odd}}\\ \delta &= (\Gamma_{\text{even}} - \Gamma_{\text{odd}})/2\\ \varepsilon &= (\Gamma_{\text{odd}} + 1)/\sqrt{2}\\ \gamma &= (\Gamma_{\text{even}} + 1)/2.\end{aligned}$$

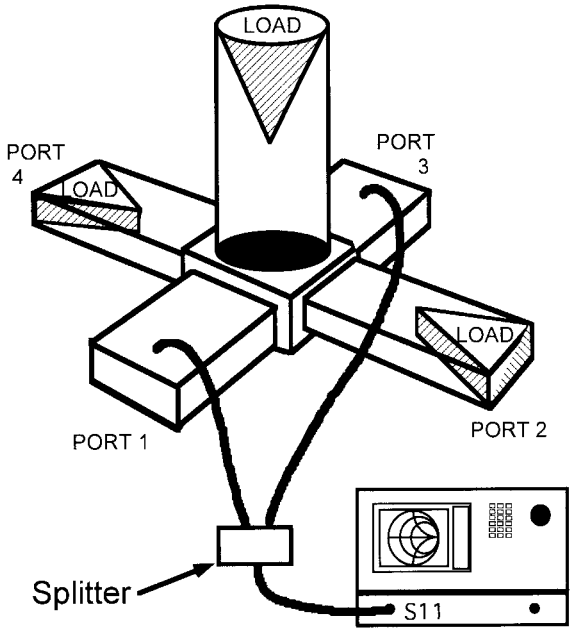

Fig. 3. Experimental arrangement for measurement of Γ_{odd} or Γ_{even} on a turnstile. For measuring Γ_{odd}, the power splitter must be a 180° splitter. For measuring Γ_{even}, the splitter must be an in-phase splitter. The dual cables from the splitter to the turnstile must be of equal phase lengths.

Dicke mentioned [1] that the turnstile may be completely described with only three independent parameters. These might be taken as $|\Gamma_{\text{even}}|$, $|\Gamma_{\text{odd}}|$, and $\measuredangle(\Gamma_{\text{even}}/\Gamma_{\text{odd}})$.

III. Resonant Disk Theory

A. Requirements

Any new turnstile design must incorporate the same device symmetry present in Dicke's turnstile (Fig. 2). This requirement brought the author to consider the waveguide disk radiator shown in Fig. 4. The disk has four coaxial feedpoints around the periphery. Such a disk can support odd- and even-mode TM resonances, making it an excellent candidate for investigation. From the previous section, it is clear that a turnstile is completely matched if $\Gamma_{\text{odd}} = \Gamma_{\text{even}} = 0$. These two requirements are considered separately in the following sections.

B. TM_{11} Disk Resonance (Odd)

Disk radiators have been well studied [5], although not inside waveguide. There are many disk resonances, but here we consider the disk TM_{nm} modes (TM with respect to the z axis, Fig. 5). The structure has been analyzed [6] and the fields beneath the disk are

$$\begin{aligned}E_z &= E_0 \cdot J_n(k\cdot\rho)\cdot\cos(n\cdot\phi)\\ H_\rho &= -(j\cdot\omega\cdot\varepsilon_0\cdot n/k^2\cdot\rho)\cdot E_0\cdot J_n(k\cdot\rho)\cdot\sin(n\cdot\phi)\\ H_\phi &= -(j\cdot\omega\cdot\varepsilon_0/k)\cdot E_0\cdot J_n'(k\cdot\rho)\cdot\cos(n\cdot\phi)\end{aligned}$$

where k is the propagation constant in the space under the disk (which we will assume to be unloaded free space), ε_0 is the permittivity of free space, J_n is the Bessel function of the first kind and order n, and the prime indicates differentiation with

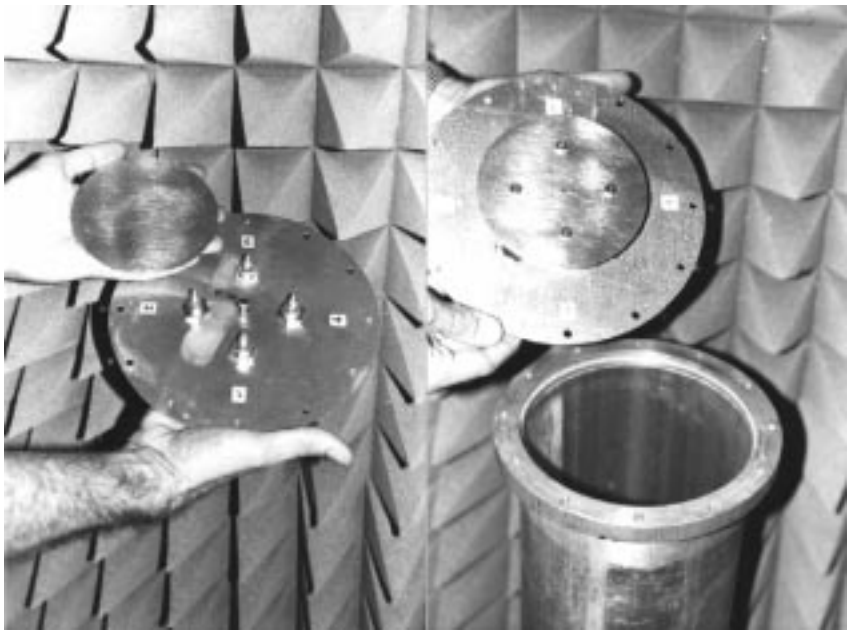

Fig. 4. Photograph of disk turnstile showing relevant geometry. There are four coaxial feed points under the disk, spaced every 90°.

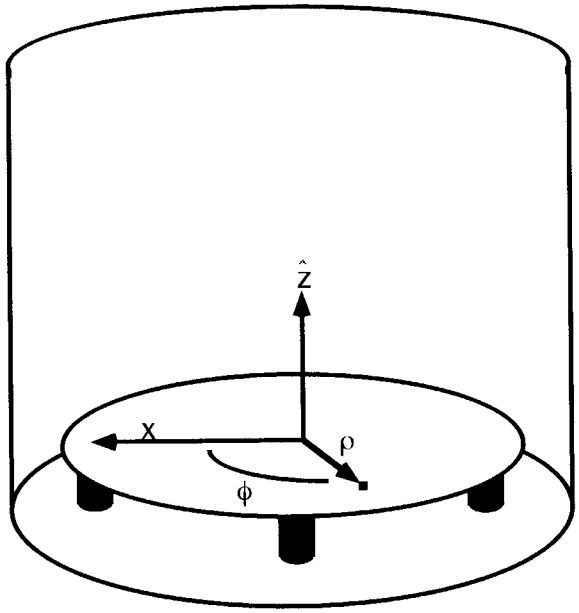

Fig. 5. Cylindrical coordinate system for disk.

respect to the argument. The voltage across the disk gap at any spot is just $E_z(\rho,\phi)\cdot d$ where d is the disk spacing ($d \ll \lambda$).

The radiation from the disk is derived from the E_z and H_ϕ transverse fields in the gap around the periphery of the disk. To find the approximate frequency of operation for a given mode, it is common to assume an open-circuited edge condition, $H_\phi(a) = 0$, so that $J_n'(ka) = 0$, where a is the radius of the disk. (In reality, one must consider radiation down the guide so that $H_\phi(a) \neq 0$). With the forgoing assumption, the resonant frequencies for the TM modes under a circular disk are

$$F_{nm} = \chi_{nm}\cdot c/2\cdot\pi\cdot a_{\text{eff}} \tag{1}$$

where χ_{nm} is the mth zero of the derivative of the Bessel function of order n, and c is the velocity of light in free space. This is often called the cavity model.

An effective radius a_{eff} somewhat larger than the actual physical radius has been introduced [7] to account for the fringing field around the edge of the disk:

$$a_{\text{eff}} = a\cdot\{1+(2\cdot d/\pi\cdot a)\cdot[\ln(\pi\cdot a/2\cdot d) + 1.7726]\}^{1/2}, \qquad a/d \gg 1. \tag{2}$$

Here we consider the TM_{11} mode resonance. This is the dominant mode for a disk, having the lowest resonance frequency, for which $\chi_{11} = 1.8412$. The magnitude of the E_z field is shown in Fig. 6(a). The field in the gap around the edge of the disk will map around the edge to couple to the TE_{11} field in the circular waveguide. This can be seen by extending the fields as in Fig. 7. The disk E_z, H_ρ, and H_ϕ fields map into the guide components E_ρ, H_z, and H_ϕ. This type of guide excitation is *mode matched* in that the disk TM_{11} fields in the gap have the same ϕ dependance as the guide TE_{11} fields. This means energy placed into the disk TM_{11} field by a coaxial probe may propagate down the guide as a TE_{11} field, which is the dominant mode for a circular guide.

C. Mathematical Model

The disk and ground plane may be regarded as a radial waveguide as in Harrington [8, pp. 208–213]. The TM_{11} field may then be represented as due to two current filaments (each radiating TM_{00} fields) placed where the coaxial probes are located. (Here we consider just one TM_{11} field due to two out-of-phase coaxial probes. More generally, there are orthogonal, degenerate TM_{11} fields which require the full set of four coaxial feed points. The extension is straight forward.) With the two probes located at radius $R < a$, as shown in Fig. 8, we may express the E_z field at any point under the disk as a

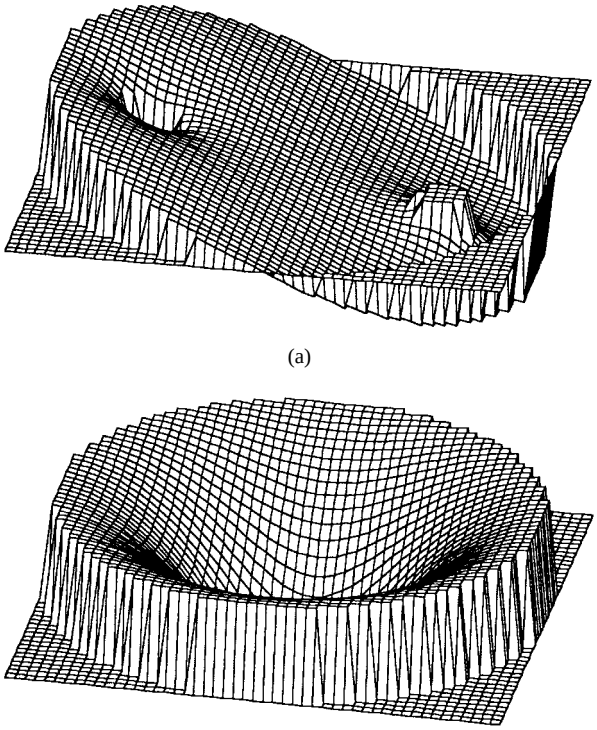

(a)

(b)

Fig. 6. (a) TM_{11} field generated by two coaxial current probes each radiating TM_{00} fields (oppositely directed). The TM_{11} field has odd symmetry with respect to rotations in ϕ. (b)TM_{01} field displayed on the same scale from the same perspective. The TM_{01} field displays even symmetry with respect to rotations in ϕ.

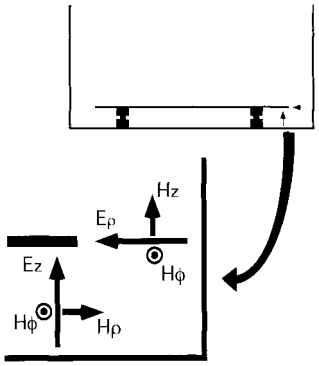

Fig. 7. Diagram showing field extension (fringing) around the edge of the disk radiator to the waveguide wall.

combination of zeroth-order Hankel functions

$$E_z(r_1,r_3)=\{\boldsymbol{A}\cdot H_0^{(1)}(k\cdot r_1)+\boldsymbol{B}\cdot H_0^{(2)}(k\cdot r_1)\}-\{\boldsymbol{A}\cdot H_0^{(1)}(k\cdot r_3)+\boldsymbol{B}\cdot H_0^{(2)}(k\cdot r_3)\}$$

where r_1 is the radius vector from one filament (port 1) and r_3 is the radius vector from the other filament (port 3). The r_1 and r_3 terms carry opposite signs because it is assumed that the filaments are driven out-of-phase to excite the TM_{11} mode (only) under the disk. The $H_0^{(1)}$ terms represent radial waves propagating toward a filament, while the $H_0^{(2)}$ terms correspond to waves traveling outward from a filament.

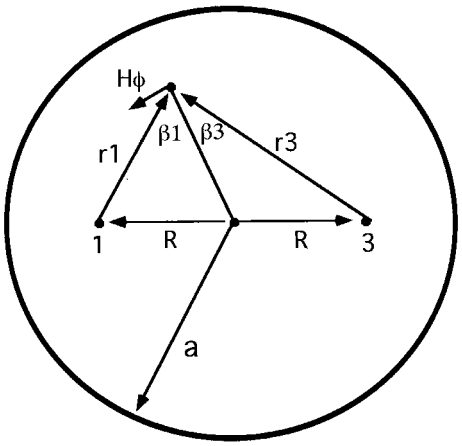

Fig. 8. Diagram showing two (of the four) coaxial feed points and vectors r_1 and r_3 used in the mathematical model. The feed points are located a distance R from the center of the disk, where $R<a=$ disk radius.

Likewise an expression may be written for the H_ϕ in terms of first-order Hankel functions

$$H_\phi(r_1,r_3)=(j/\eta)\{[\boldsymbol{A}\cdot H_1^{(1)}(k\cdot r_1)+\boldsymbol{B}\cdot H_1^{(2)}(k\cdot r_1)]\cdot\cos\beta_1-[\boldsymbol{A}\cdot H_1^{(1)}(k\cdot r_3)+\boldsymbol{B}\cdot H_1^{(2)}(k\cdot r_3)]\cdot\cos\beta_3\}.$$

The cosine terms are necessary to take the projection in the ϕ direction. The quantity η is the impedance of the space under the disk. For completeness, the Hankel functions are defined as

$$\begin{aligned}H_0^{(1)}&=J_0(x)+j\cdot N_0(x)\\H_0^{(2)}&=J_0(x)-j\cdot N_0(x)\\H_1^{(1)}&=J_1(x)+j\cdot N_1(x)\\H_1^{(2)}&=J_1(x)-j\cdot N_1(x)\end{aligned}$$

where J_0 and J_1 are the zeroth- and first-order Bessel functions of the first kind, and N_0 and N_1 are the zeroth- and first-order Bessel functions of the second kind.

The complex ratio $\boldsymbol{A}/\boldsymbol{B}$ is the important factor in determining the net impedance at either of the two drive points. Without loss of generality, we let $\boldsymbol{B}=1$ and express the feed-point drive impedance in terms of $\boldsymbol{A}$ alone.

Before proceeding, we must know the value of E_z/H_ϕ somewhere under the disk. In the gap at the edge of the disk we may make some assumptions about the radiation into the guide to develop an impedance boundary condition. In a very specific way, the gap looks like an *infinite slot* radiator, in that E_z and H_ϕ are always orthogonal, there is never a component of E along the guide, and there is no end to the gap. Without further justification, we have used the conductance and susceptance (per unit length) for a radiating infinite slot developed by Harrington [8, pp. 180–183]:

$$\begin{aligned}G&=(\pi/\eta\cdot\lambda)\cdot[1-(k\cdot d)^2/24]\\B&=(1/\eta\cdot\lambda)\cdot[3.135-2\cdot\log(k\cdot d)],\qquad d/\lambda<0.1.\end{aligned}$$

The gap is capacitive, since B is always positive. For a gap width d, the voltage across the gap (ignoring fringing) is

$$V=E_z\cdot d.$$

With the voltage and the assumed gap admittance, we can write H_ϕ at the edge of the disk as

$$H_\phi|_{\text{edge}} = V \cdot (G + j \cdot B) = E_z \cdot d \cdot (G + j \cdot B).$$

Therefore

$$E_z / H_\phi|_{\text{edge}} = 1/d \cdot (G + j \cdot B)$$

where it is understood that the η dependance in the G and B expressions will now be the TE_{11} guide impedance.

Accordingly, assuming Harrington's gap admittance, we can determine values for the coaxial-probe drive impedance (real and reactive) for out-of-phase drive using the Hankel function expressions above. Let the point of interest approach the feedpost of port 1. The total disk voltage there is $V_{\text{total}} = E_z \cdot d$, with E_z as given before. The total current for port 1 is

$$I_{\text{total}} = 2 \cdot \pi \cdot r \cdot H_\phi$$

where r is the radius of a small integrating path around port 1 (allowed to approach the physical radius of the coaxial post). The impedance at port 1 is then $Z_{\text{port 1}} = V_{\text{total}}/I_{\text{total}}$. Note that feedpost 3 cannot induce any current in feedpost 1. This makes the integral particularly simple.

The above model for Γ_{odd} is complete except for the inductive reactance of the feedposts themselves. This may be accounted for in an *ad hoc* manner by simply adding the estimated post reactance to the impedance calculated above. The inductance per unit length for a cylinder [9] is

$$\mathcal{L} = (\mu/2 \cdot \pi) \cdot \ln(\lambda/2 \cdot \pi \cdot r)$$

where μ is the permeability of free space and r is the radius of the feedpost. Accordingly, for a gap separation of d, the feedpost reactance is

$$\begin{aligned} X_{\text{feedpost}} &= j \cdot 2 \cdot \pi \cdot F \cdot L = j \cdot 2 \cdot \pi \cdot F \cdot (d \cdot \mathcal{L}) \\ &= j \cdot F \cdot d \cdot \mu \cdot \ln(\lambda/2 \cdot \pi \cdot r). \end{aligned}$$

This amounts to some $40j\Omega$ to $80j\Omega$ for the designs considered here.

D. TM_{01} Disk Resonance (Even)

Consider the TM_{01} mode resonance as shown in Fig. 6(b). From (1), the resonant frequency for the TM_{01} mode goes as $\chi_{01} = 3.8317$. Recall that $\chi_{11} = 1.8412$. Accordingly, the ratio of the natural resonance frequencies of these two modes is $3.8317/1.8412 = 2.0811$. Is it possible then, that these disk resonances might be made to occur at the same frequency?—in fact, yes it is. It is only necessary to place a central padding capacitance between the disk and the ground plane in order to lower the frequency of the TM_{01} mode. By placing the capacitor at the center of the disk, it cannot impact the TM_{11} resonance, because the TM_{11} resonance never has any field at the disk center.

The TM_{01} mode is even as there is no field variation with ϕ, as seen in Fig. 6(b).

It is a simple matter to determine how much capacitive reactance is necessary to lower the TM_{01} resonance to a given frequency. Consider the disk with no feed points and only the central capacitance. We may express the fields as

$$\begin{aligned} E_z &= \boldsymbol{A} \cdot H_0^{(1)}(k \cdot r) + H_0^{(2)}(k \cdot \rho) \\ H_\phi &= (j/\eta) \cdot \{\boldsymbol{A} \cdot H_1^{(1)}(k \cdot \rho) + H_1^{(2)}(k \cdot \rho)\}, \qquad (\boldsymbol{B} = 1). \end{aligned}$$

If we apply the *open-circuited* edge condition, we have $H_\phi(a) = 0$. This determines complex constant $\boldsymbol{A}$ (for a given disk radius a and gap spacing d) and determines the resultant impedance at the central capacitor (pseudo feedpoint). That is, once again we have

$$V_{\text{cap}} = E_z \cdot d \quad \text{and} \quad I_{\text{cap}} = 2 \cdot \pi \cdot r \cdot H_\phi(r).$$

So that $Z_{\text{cap}} = V_{\text{cap}}/I_{\text{cap}}$, which we set equal to $j \cdot X_{\text{cap}}$ and solve for the resonance frequency. Indeed, by using a large capacitor ($X_{\text{cap}} \to 0$), the resonance frequency may ultimately be lowered by a factor of 4.5 (well below the resonance of the disk TM_{11} mode).

With the TM_{01} mode operating in this fashion (i.e., with a central padding capacitor), the resonances may be made coincident. The TM_{01} (even mode) should be self matching in the sense that the voltage applied at ports 1 and 3 will appear at ports 2 and 4 due to the symmetry of the mode. If ports 2 and 4 are terminated in 50 Ω each, we may expect 50 Ω to be reflected to ports 1 and 3. However, this does not account for the feedpost inductance. A more complete model is shown in Fig. 9(a) where the four feedposts are shown radiating from a common node (since the disk voltage $E_z \cdot d$ is the same at all four posts). The disk resonance, augmented by the central capacitor, is shown as a parallel *LC* circuit. If the disk resonance is tuned below the frequency of operation, it will provide a net capacitive reactance, as shown in Fig. 9(b). In Fig. 9(c), ports 1 and 3 are pulled to the left and ports 2 and

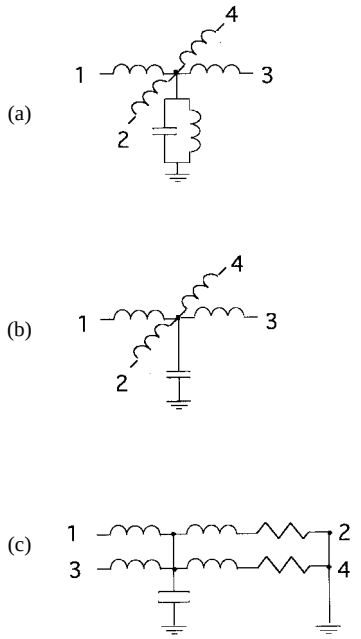

Fig. 9. Circuit model showing how the feedpost inductance can be absorbed in the even-mode response.

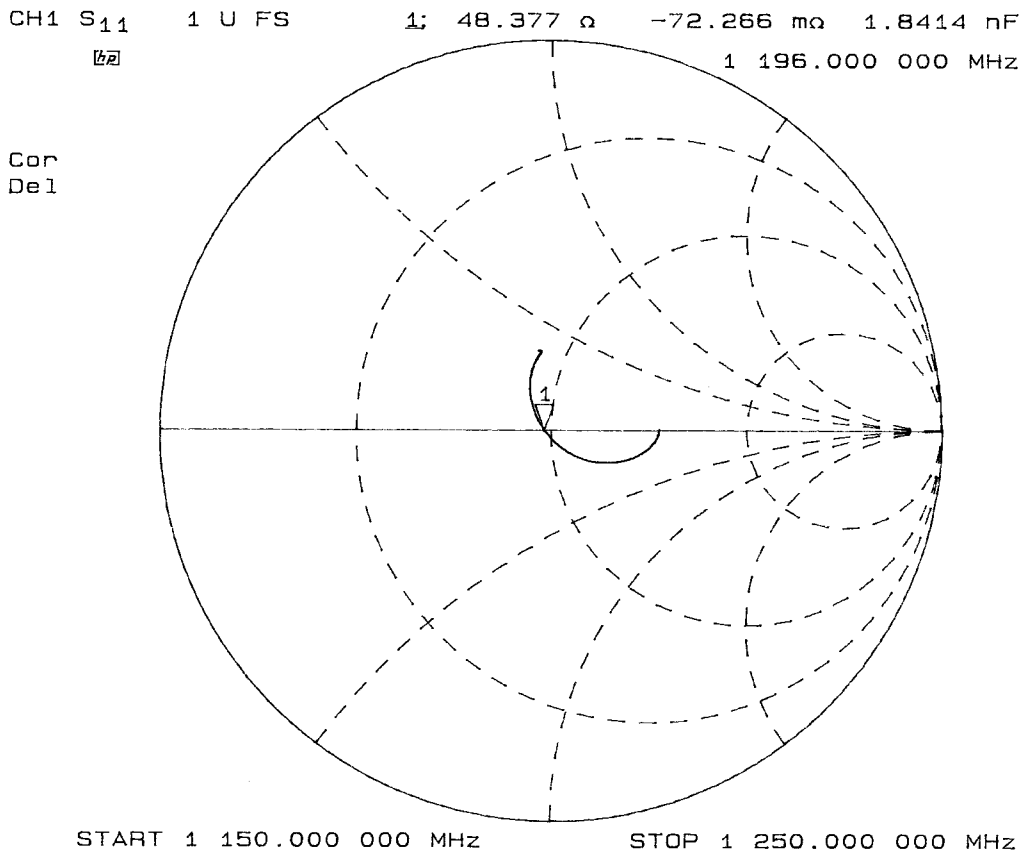

(a)

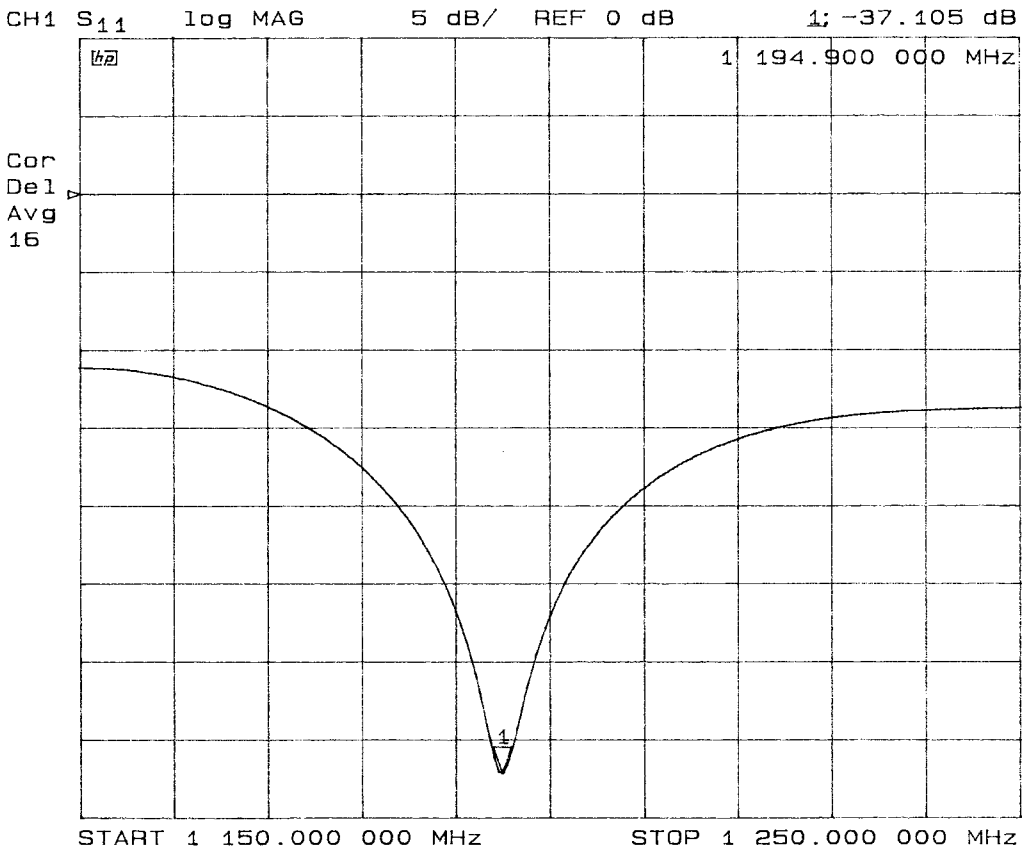

(b)

Fig. 10. (a) and (b) Measured Γ_{odd} data for L-band prototype.

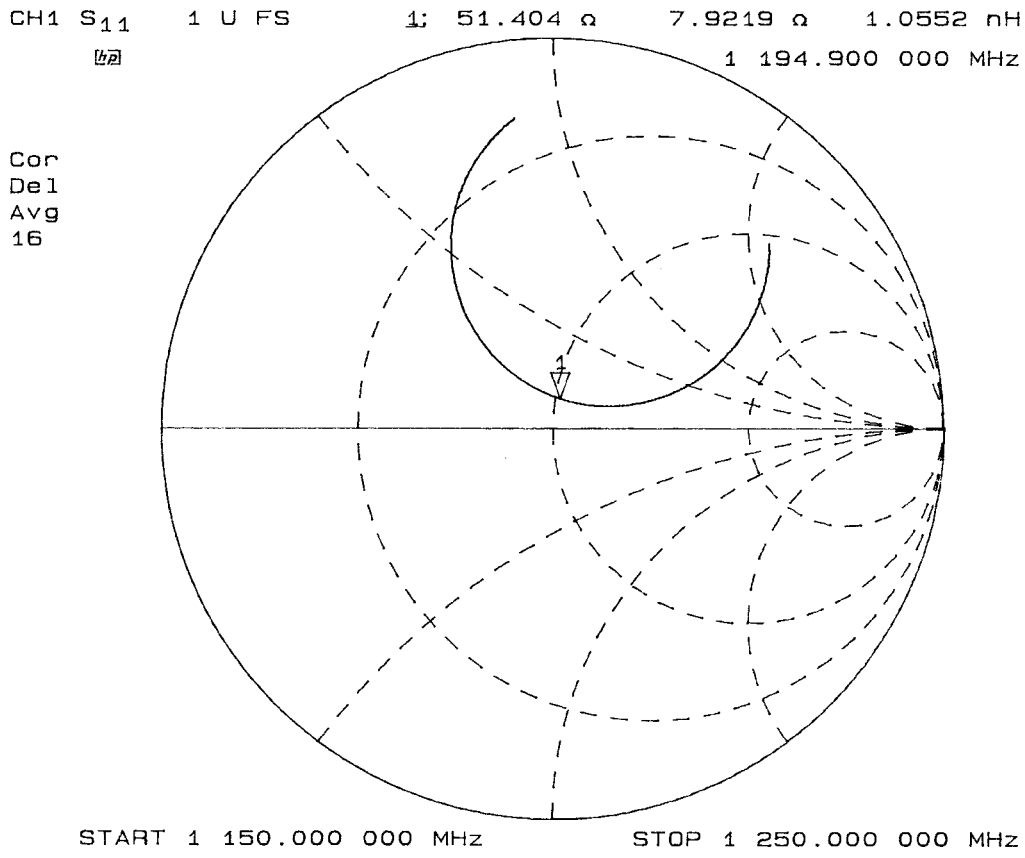

(c)

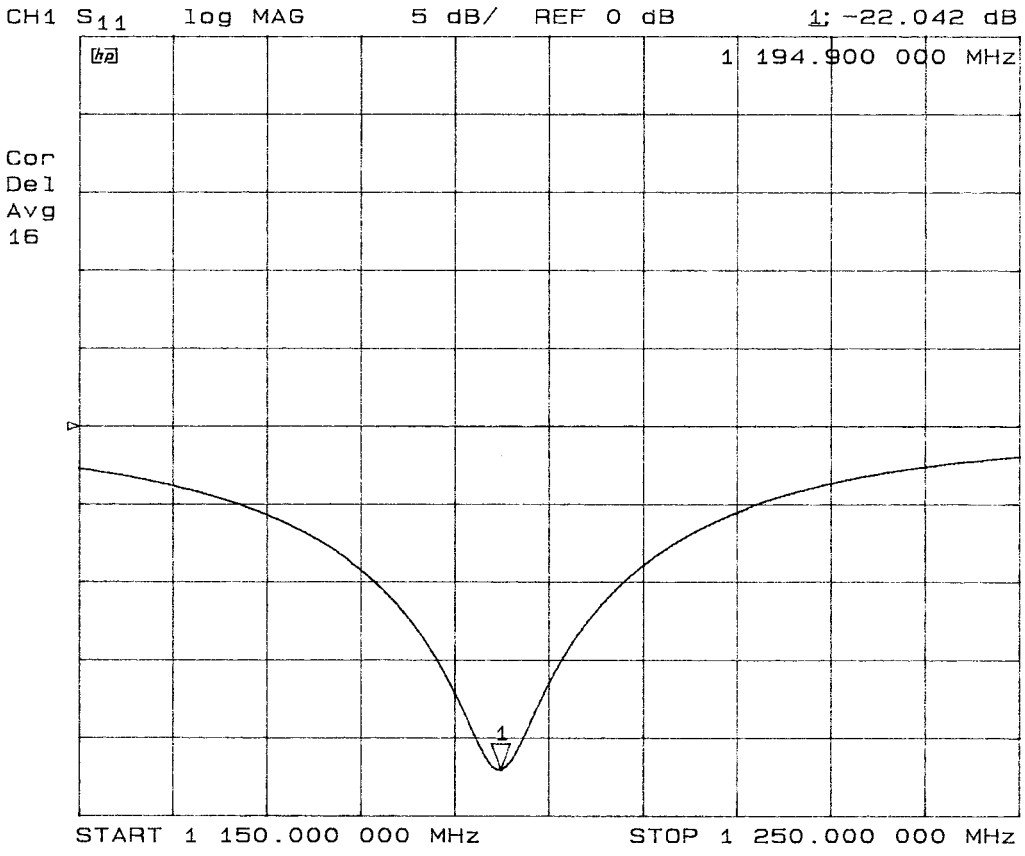

(d)

Fig. 10. *(Continued.)* (c) and (d) Measured Γ_{even} data for L-band prototype.

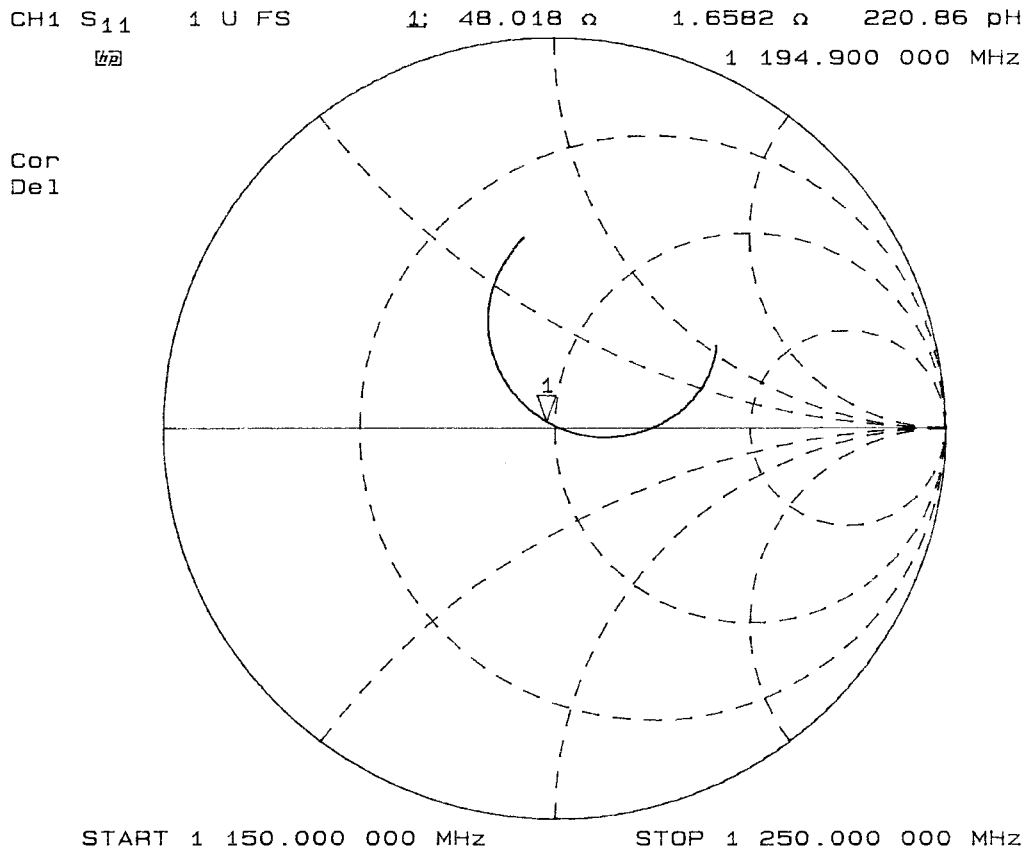

(e)

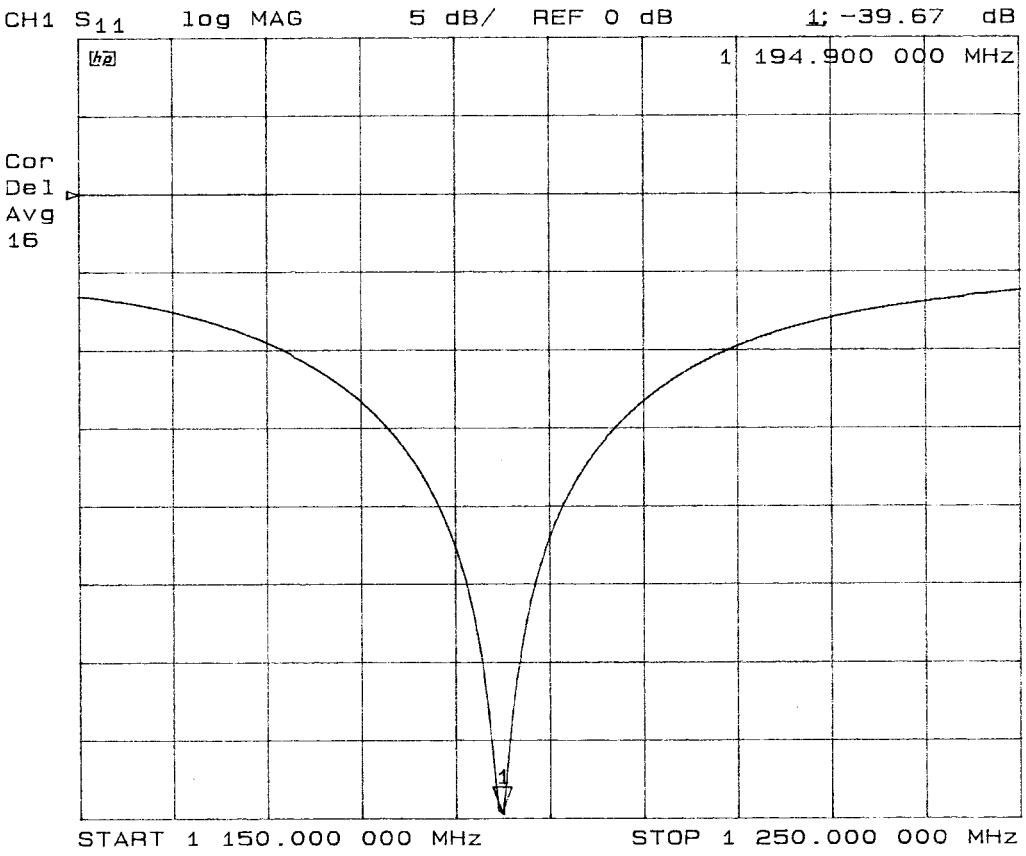

(f)

Fig. 10. *(Continued.)* (e) and (f) Measured Γ_{total} at port 1 for the L-band prototype.

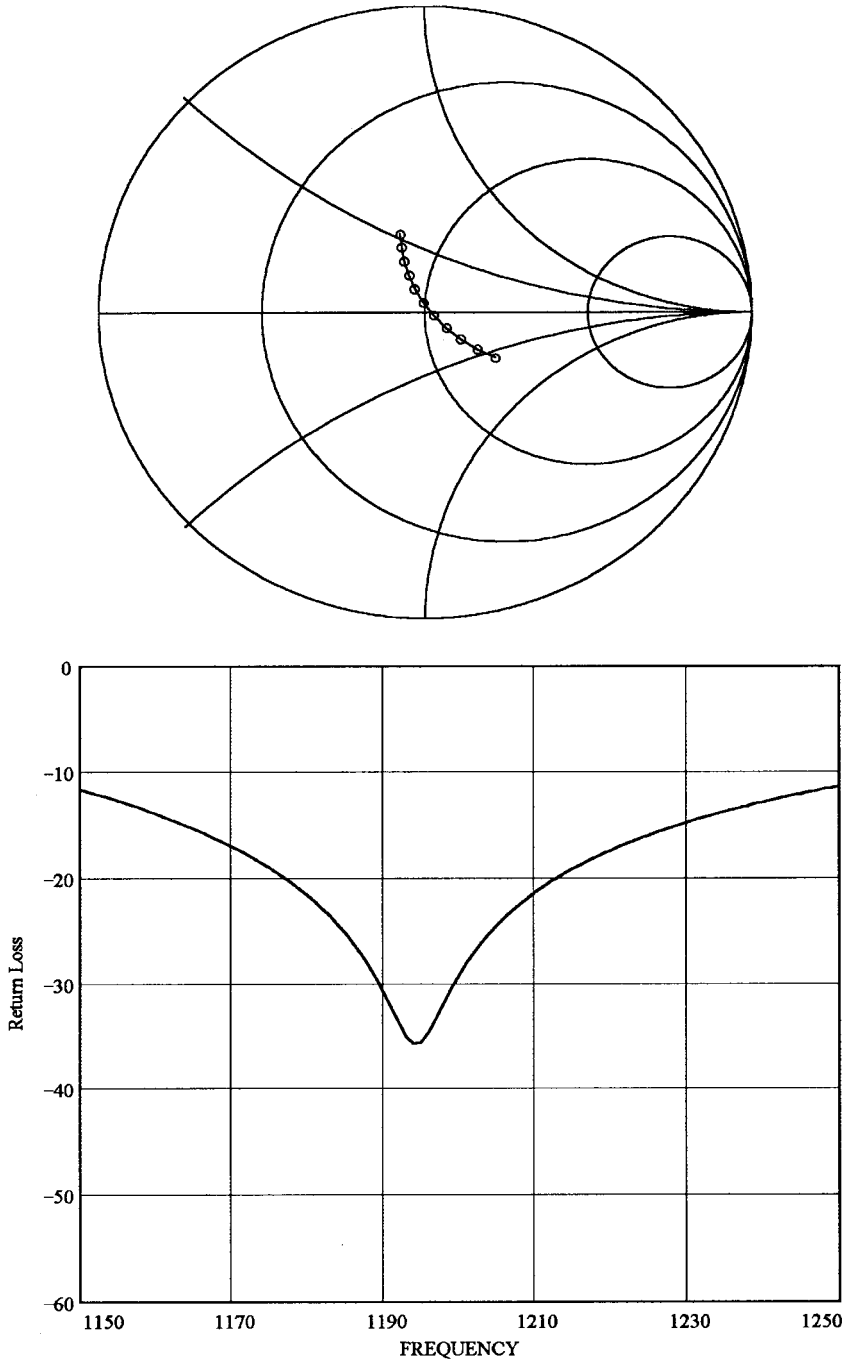

Fig. 11. Modeled Γ_{odd} performance where the effective disk radius is enlarged to 8.2 cm from the physical value of 6.1 cm to account for field fringing around the disk to the guide walls.

4 (loaded with 50 Ω) are pulled to the right. To first order, the disk resonance can always be adjusted to absorb the feedpost reactance and yield 50 Ω at ports 1 and 3.

We may summarize the odd and even modes as follows. By driving the turnstile in an *odd* manner, disk TM_{11} mode will be excited and a traveling TE_{11} wave will propagate down the circular waveguide. By driving the turnstile in an *even* manner, disk TM_{01} will be excited, coupling all four of the coaxial ports in-phase (at center frequency). And in point, if a single coaxial port is driven (port 1, 2, 3, or 4) the principle of superposition indicates both modes will be equally excited, as follows:

$$\underset{\substack{\text{single port}\\ \text{drive}}}{\begin{bmatrix}1\\0\\0\\0\\0\\0\end{bmatrix}} = \underset{\substack{\text{odd}\\ \text{drive}}}{\begin{bmatrix}\frac{1}{2}\\0\\-\frac{1}{2}\\0\\0\\0\end{bmatrix}} + \underset{\substack{\text{even}\\ \text{drive}}}{\begin{bmatrix}\frac{1}{2}\\0\\\frac{1}{2}\\0\\0\\0\end{bmatrix}}.$$

Only one precaution must be observed. The disk must operate above the waveguide TE_{11} cutoff and below the waveguide TM_{01} cutoff. This ensures that the disk TM_{11}

TABLE I

Center frequency of operation	= 1195 MHz
Radius of circular waveguide	= 8.70 cm
TE_{11} cutoff frequency	= 1011 MHz
TM_{01} cutoff frequency	= 1320 MHz
Radius of disk (physical)	= 6.1 cm
Radial location of feed posts	= 3.5 cm
Radius of coaxial feed posts	= 0.35 cm
Disk spacing	= 2.2 cm
Center loading capacitor	= 1.5 pF

mode *will* radiate and that the disk TM_{01} mode *cannot* radiate (and only serves to couple the four coaxial ports).

IV. Experimental Prototype

An experimental prototype was constructed for L-band. The dimensions are listed in Table I.

The Γ_{odd} response is shown in Fig. 10(a) and (b). A drive impedance of 50 Ωm occurred at 1195 MHz ($\Gamma_{\text{odd}} = -37$ dB). Γ_{odd} was measured using a Mini-Circuits Laboratory ZAPDJ-2 180° coaxial power splitter with equal-length cables. Coaxial ports 1 and 3 were driven, with the circular waveguide terminated. Ports 2 and 4 are isolated, but were also terminated. The phase reference plane here and in all following plots was coincident with the ground plane under the disk.

The Γ_{even} response is shown in Fig. 10(c) and (d). The central capacitor was adjusted to bring the TM_{01} response to 1195 MHz ($C = 1.5$ pF). Coaxial ports 1 and 3 were driven, with ports 2 and 4 terminated in 50-Ωm loads. The waveguide ports 5 and 6 are isolated ports, but were also terminated. Γ_{even} was measured using a Mini-Circuits ZAPD-2 in-phase coaxial power splitter.

The total reflection coefficient for port 1 (or port 2, 3, and 4) is shown in Fig. 10(e) and (f), and is in good agreement with the Γ_{odd} and Γ_{even} data. Recall that

$$\Gamma_{\text{total}} = \alpha = (\Gamma_{\text{even}} + \Gamma_{\text{odd}})/2.$$

Accordingly, Fig. 10(c) should be the mean of Fig. 10(a) and 10(b), which appears to be the case.

The mathematical model showed reasonable agreement with Γ_{odd} when the effective disk radius a_{eff} was extended from the physical value of $a = 6.1$ cm to a *fringed* value of 8.2 cm. This is certainly realistic since the fringed value for the disk over a ground plane (using formula two) is 8.1 cm. The modeled Γ_{odd} is shown in Fig. 11. The model predicts the actual resonance but fails to yield the tight locus seen in Fig. 10(a) and (b).

V. Prospectus

The resonant disk turnstile shows a useful fractional bandwidth of about 3% compared with a Dicke turnstile bandwidth of closer to 6%. Accordingly, the new turnstile will not make Dicke's invention obsolete, but should be considered for any narrow-band application. The two turnstiles (L-band) are shown in Fig. 12 for a realistic size comparison.

The disk turnstile can readily be used as a circular polarizer. It is only necessary to add two shorting coaxial cable stubs to ports 2 and 4. The total stub lengths should be $\lambda/8$ and $3\lambda/8$, so that signals reflected from the stubs to ports 2 and 4 will be out-of-phase with each other (and in quadrature with port 1 and 3). For low-power work, an open and shorted stub (both of length $\lambda/8$) would suffice.

Fig. 12. Photograph comparing the size of an L-band disk turnstile with Dicke's full waveguide turnstile.

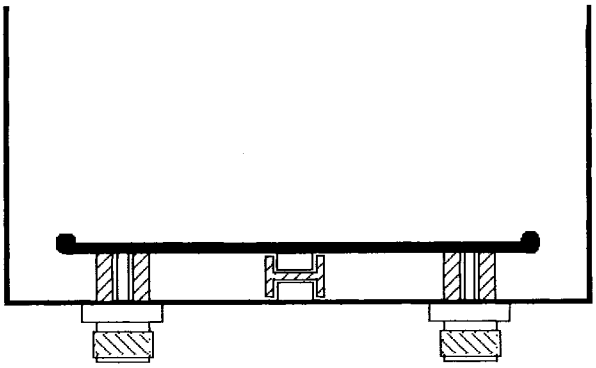

Fig. 13. Proposed modifications for a disk turnstile to permit high-power operation. The four probes have coaxial dielectric collars. The central padding capacitor has a dielectric spacer with collar. The edge of the disk is rounded to prevent arcing.

The disk turnstile would be excellent for high-power radar work. The total applied voltage to a coaxial feed (assuming the feedpoint near the disk edge) appears across the disk gap. Fig. 13 shows how a disk turnstile can be modified to withstand high-power levels by incorporating dielectric material (around the feed points and at the central capacitor), and by using a rounded disk edge.

VI. Summary

A new type of turnstile has been presented—the resonant disk turnstile—which is simple to analyze as well as simple to construct. An L-band prototype unit displayed reasonable agreement with theory. The region of operation for a disk turnstile lies between the circular waveguide TE_{11} cutoff and the TM_{01} cutoff. Dimensions provided for the prototype may easily be scaled for other wavelengths. Using 0° and 180° power splitters with a network analyzer allows the operation of the disk TM_{01} and TM_{11} modes, respectively, to be checked, thereby completely describing the system. The L-band unit described herein should be able to handle power levels well beyond that of any 50-Ω·m feeder cable.

VII. Dedication and Acknowledgment

With this paper, the author would like to honor the memory and spirit of Robert Dicke (1916–1997). The author is indebted to Arecibo Observatory, National Astronomy & Ionosphere Center (N.A.I.C.), PR, for time and facilities to develop the disk turnstile. Helpful discussion and correspondence were received from J. Hagen and G. Lauria, N.A.I.C. Cornell University operates N.A.I.C. under a cooperative agreement with the National Science Foundation. Patent information is available from Cornell Research Foundation, Inc., 20 Thornwood Drive, Suite 105, Ithaca, NY 14850 USA.

References

[1] C. G. Montgomery, R. H. Dicke, and E. M. Purcell, *Principles of Microwave Circuits*, (Radiation Lab. Series, vol. 8). New York: McGraw-Hill, 1948, pp. 459–466.

[2] G. L. Ragan, *Microwave Transmission Circuits*, (Radiation Lab. Series, vol. 9), New York: McGraw-Hill, 1948, pp. 375–377.

[3] M. A. Meyer and H. B. Goldberg, "Applications of the turnstile junction," *Trans. IRE Microwave Theory Tech.*, vol. MTT-3, pp. 40–45, Dec. 1955.

[4] R. H. Dicke, "Turnstile junction for producing circularly polarized waves," U.S. Patent 2 686 901, Aug. 17, 1954.

[5] A. G. Derneryd, "Analysis of the microstrip disk antenna element," *IEEE Trans. Antennas Propagat.*, vol. AP-27, pp. 660–664, Sept. 1979.

[6] J. Watkins, "Circular resonant structures in microstrip," *Electron. Lett.*, vol. 5, pp. 524–525, Oct. 1969.

[7] L. C. Shen *et al.*, "Resonant frequency of a circular disk, printed-circuit antenna," *IEEE Trans. Antennas Propagat.*, vol. AP-25, pp. 595–596, July 1977.

[8] R. F. Harrington, *Time-Harmonic Electromagnetic Fields*. New York: McGraw-Hill, 1961.

[9] E. C. Jordan and K. G. Balmain, *Electromagnetic Waves and Radiating Systems*. Englewood Cliffs, NJ: Prentice-Hall, 1968, p. 561.

Robert K. Zimmerman, Jr., (S'78–M'78) was born in Illinois on August 13, 1951. He received the B.S. and M.S. degrees in physics from Southern Illinois University at Edwardsville, in 1973 and 1975, respectively, and the M.S.E.E. degree in electrical engineering from the University of Illinois at Champaign-Urbana, in 1980.

In 1978, he worked for the Watkins-Johnson Company, building some of the first commercial GaAs FET amplifiers. In 1979, he began working for Cornell University at the Arecibo Observatory, Arecibo, PR, as a Receiver Circuits Engineer. In 1986, he joined the NASA Goddard Spaceflight Center working in free-space laser communication. He spent two years as a Transmitter Engineer for the Voice of America, Greenville, NC, and since 1994, has headed the transmitter group at the Arecibo Observatory. His current interest is in waveguide devices.